

Self-similarity of higher-order moving averages

Sergio Arianos,^{1,2} Anna Carbone,^{1,3} and Christian Türk¹¹*Physics Department, Politecnico di Torino, Corso Duca degli Abruzzi 24, I-10129 Torino, Italy*²*Antenna and Electromagnetic Compatibility Lab (LACE), Politecnico di Torino, I-10129 Torino, Italy*³*ETH Zurich, CLU, Clausiusstrasse 50, CH-8092 Zurich, Switzerland*

(Received 22 June 2011; revised manuscript received 2 October 2011; published 24 October 2011)

In this work, higher-order moving average polynomials are defined by straightforward generalization of the standard moving average. The self-similarity of the polynomials is analyzed for fractional Brownian series and quantified in terms of the Hurst exponent H by using the detrending moving average method. We prove that the exponent H of the fractional Brownian series and of the detrending moving average variance asymptotically agree for the first-order polynomial. Such asymptotic values are compared with the results obtained by the simulations. The higher-order polynomials correspond to trend estimates at shorter time scales as the degree of the polynomial increases. Importantly, the increase of polynomial degree does not require to change the moving average window. Thus trends at different time scales can be obtained on data sets with the same size. These polynomials could be interesting for those applications relying on trend estimates over different time horizons (financial markets) or on filtering at different frequencies (image analysis).

DOI: [10.1103/PhysRevE.84.046113](https://doi.org/10.1103/PhysRevE.84.046113)

PACS number(s): 89.65.Gh, 05.45.Tp, 89.75.Da

I. INTRODUCTION

Statistical physics is increasingly recognized and explored for unraveling complexity in diverse systems. Self-similarity and long-range correlations have been investigated in financial series [1–7], other than in systems as biological and physiological [8–11], solar, geophysical, environmental, and solid state [12–16]. In particular, stock markets are complex dynamical systems operating in synchronization to other social activities. Thus financial time series exhibit patterns related to such activities, which are under intense investigation by statistical physics approaches. Technical traders sell and buy stocks near the top and close to the bottom of the trend. Occurrence of maximum and minimum of the price trend and trend reversal trigger trading decisions. The golden cross (buy stocks) and dead cross (sell stocks) rule exploits the intersections of long-term and short-term moving averages by adjusting the moving average window n to the characteristic behavior of a particular stock market. Technical rules based on moving averages are under continuous investigation and improvement [4–7]. Correlations are quantified in terms of scaling exponents by using estimators suitably defined for such systems [17–20]. For nonstationary time series, the detrended fluctuation analysis (DFA) [21–27], the rescaled range statistical analysis (R/S), and the detrending moving average analysis (DMA) [28–31] can be adopted to explore long-range autocorrelations, multifractal features [32–37], cross correlation [38,39], and higher dimensional fractals [40–42]. The DMA algorithm operates through the estimate of a generalized variance of the long-range correlated series $y(i)$ around the moving average:

$$\tilde{y}_n(i) = \frac{1}{n} \sum_{k=0}^{n-1} y(i-k), \quad (1)$$

with n the moving average window. The reference point of the moving average window can be changed by the introduction of a parameter θ with $0 \leq \theta \leq 1$. Accordingly, Eq. (1), which corresponds to $\theta = 0$, is generalized as

$\tilde{y}_n(i) = 1/n \sum_{k=-\theta n}^{n-1-\theta n} y(i-k)$. By repeating the calculation for different values of the window n , the power law dependence of the generalized variance σ_{DMA} is obtained:

$$\sigma_{\text{DMA}}^2 \sim n^{2H}, \quad (2)$$

where H is the Hurst exponent which is related to the correlation properties of $y(i)$ ($H = 0.5$, $H < 0.5$ and $H > 0.5$ hold for uncorrelated, negatively, and positively correlated signals, respectively).

The DMA algorithm is a remarkable example of integration between finance tools and complex system concepts. Self-similarity and long-range correlations are estimated by means of a generalized variance around the moving average, which is a popular instrument of technical analysis.

In this work, a generalization of Eq. (1) is proposed and higher-order moving average polynomials are introduced. The scaling behavior of such polynomials is then investigated by means of the detrending moving average algorithm (Sec. II). Furthermore, it is analytically proved that the asymptotic behavior of the exponents H of the moving average polynomials and of the detrending moving average variance agree. This implies that the application of the DMA method does not alter the value of H at large n (Sec. III). Finally, we note that the higher-order polynomials correspond to estimates of trends at smaller and smaller time scales: as the degree of the polynomial increases (decreases), more (less) low-frequency components are filtered out. The advantage of the proposed approach is to operate at constant value of the moving average window n . Thus trends at different time spans are calculated over data set with the same size. These polynomials could improve the accuracy of trends estimated over different space or time horizons.

II. HIGHER-ORDER MOVING AVERAGE POLYNOMIALS

The proposed procedure is based on a generalization of the least-square method, which is commonly applied for the best fit of random data by minimizing the sum of the squares

of the deviations of a set of N data points, with respect to a polynomial $\hat{y}_m(i)$ of degree m . For a first degree polynomial $\hat{y}_1(i) = a_0 + a_1 i$, the coefficients a_0 and a_1 that minimize the sum of the squares, are

$$a_1 = \frac{\sum_{i=1}^N y(i)i - \frac{1}{N} \sum_{i=1}^N i \sum_{i=1}^N y(i)}{\sum_{i=1}^N i^2 - \frac{1}{N} \left(\sum_{i=1}^N i \right)^2}, \quad (3a)$$

$$a_0 = \frac{1}{N} \sum_{i=1}^N y(i) - a_1 \frac{1}{N} \sum_{i=1}^N i. \quad (3b)$$

One can note that the moving average defined by Eq. (1) can be obtained by Eq. (3b) when the sum is performed over a moving window of size n rather than over the whole data set N and $a_1 = 0$. Therefore, one can generalize Eqs. (3a) and (3b) with the sum calculated over a moving window:

$$\begin{aligned} \tilde{a}_{n,1}(i) &= \frac{\sum_{k=0}^{n-1} y(i-k)(i-k) - \frac{1}{n} \sum_{k=0}^{n-1} y(i-k) \sum_{h=0}^{n-1} (i-h)}{\sum_{k=0}^{n-1} (i-k)^2 - \frac{1}{n} \left[\sum_{k=0}^{n-1} (i-k) \right]^2}, \end{aligned} \quad (4a)$$

$$\tilde{a}_{n,0}(i) = \frac{1}{n} \sum_{k=0}^{n-1} y(i-k) - \frac{1}{n} \tilde{a}_{n,1}(i) \sum_{k=0}^{n-1} (i-k). \quad (4b)$$

The quantities $\tilde{a}_{n,0}(i)$ and $\tilde{a}_{n,1}(i)$ are function of i , as opposed to a_0 and a_1 in Eqs. (3a) and (3b) which are constant. One can note that if $\tilde{a}_{n,1}(i)$ is zero, Eq. (4b) coincides with Eq. (1). By using Eqs. (4a) and (4b), the first order moving average polynomial can be written as

$$\tilde{y}_n(i) = \tilde{a}_{n,0}(i) + \tilde{a}_{n,1}(i)i. \quad (5)$$

Furthermore, we observe that the reference point of the moving average window may be changed to any point within the window n by the introduction of a parameter θ with $0 \leq \theta \leq 1$. The general expressions of $\tilde{a}_{n,0}(i)$ and $\tilde{a}_{n,1}(i)$ with the sum extremes depending on θ are written in the Appendix.

By following the approach described above, higher-order moving average polynomials of the form

$$\tilde{y}_n(i) = \tilde{a}_{n,0}(i) + \tilde{a}_{n,1}(i)i + \dots + \tilde{a}_{n,m}(i)i^m \quad (6)$$

can be thus generated, where the coefficients $\tilde{a}_{n,0}(i)$, $\tilde{a}_{n,1}(i)$, \dots , $\tilde{a}_{n,m}(i)$ are obtained by generalizing the corresponding terms of the least-square expansion. Higher-order moving average polynomials, defined by Eq. (6), have been simulated by means of artificial long-range correlated series with scaling exponent H by the random midpoint displacement (RMD) and the Cholesky-Levinson factorization (CLF) algorithms [43]. Moving average polynomials of order $m = 0$, $m = 1$, $m = 2$, and $m = 3$ are shown in Fig. 1 with window size $n = 400$ referred to the midpoint of the window ($\theta = 0.5$). One can note that the fit improves for higher order polynomials. Next, we consider the variance

$$\sigma_{\text{DMA}}^2 = \frac{1}{N-n} \sum_{i=n}^N [y(i) - \tilde{y}_n(i)]^2, \quad (7)$$

where $y(i)$ is a long-range correlated series with Hurst exponent H . The log-log plots of σ_{DMA}^2 vs n for $m = 0$, $m = 1$, $m = 2$, and $m = 3$ are shown in Fig. 2. The polynomials are calculated for artificial series generated by the RMD method and are centered in the first ($\theta = 1$), in the middle ($\theta = 0.5$), and in the last ($\theta = 0$) point of the window. The

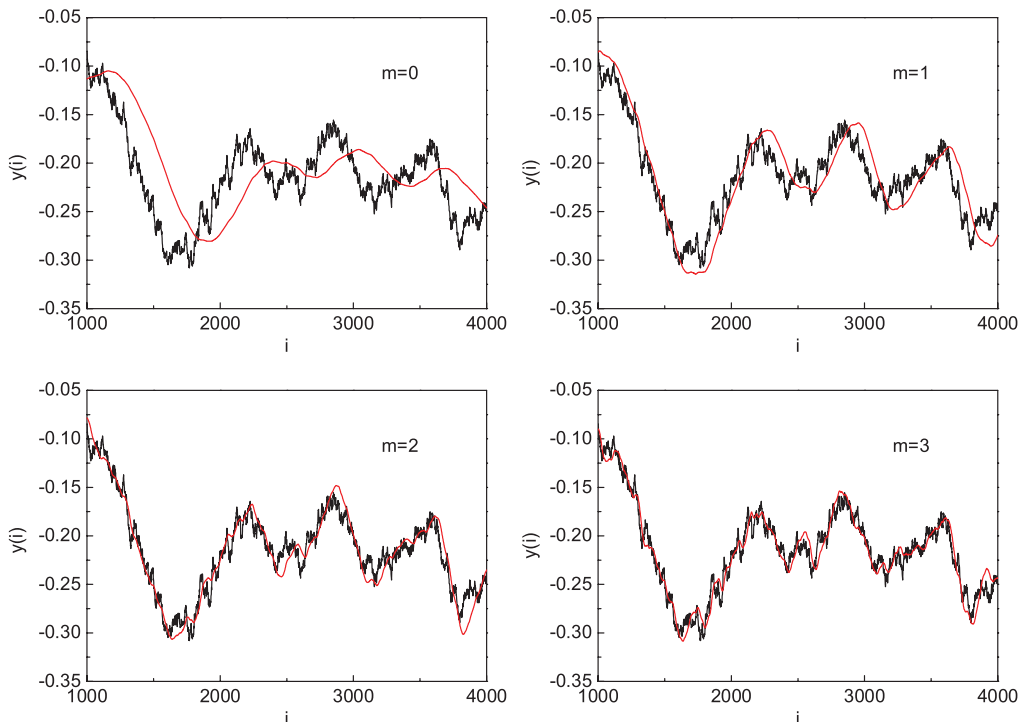


FIG. 1. (Color online) Moving average polynomials of degree $m = 0$, $m = 1$, $m = 2$, and $m = 3$ for self-similar series with Hurst exponent $H = 0.5$ generated by the random midpoint displacement algorithm. The window size is $n = 400$ and the reference is $\theta = 0.5$.

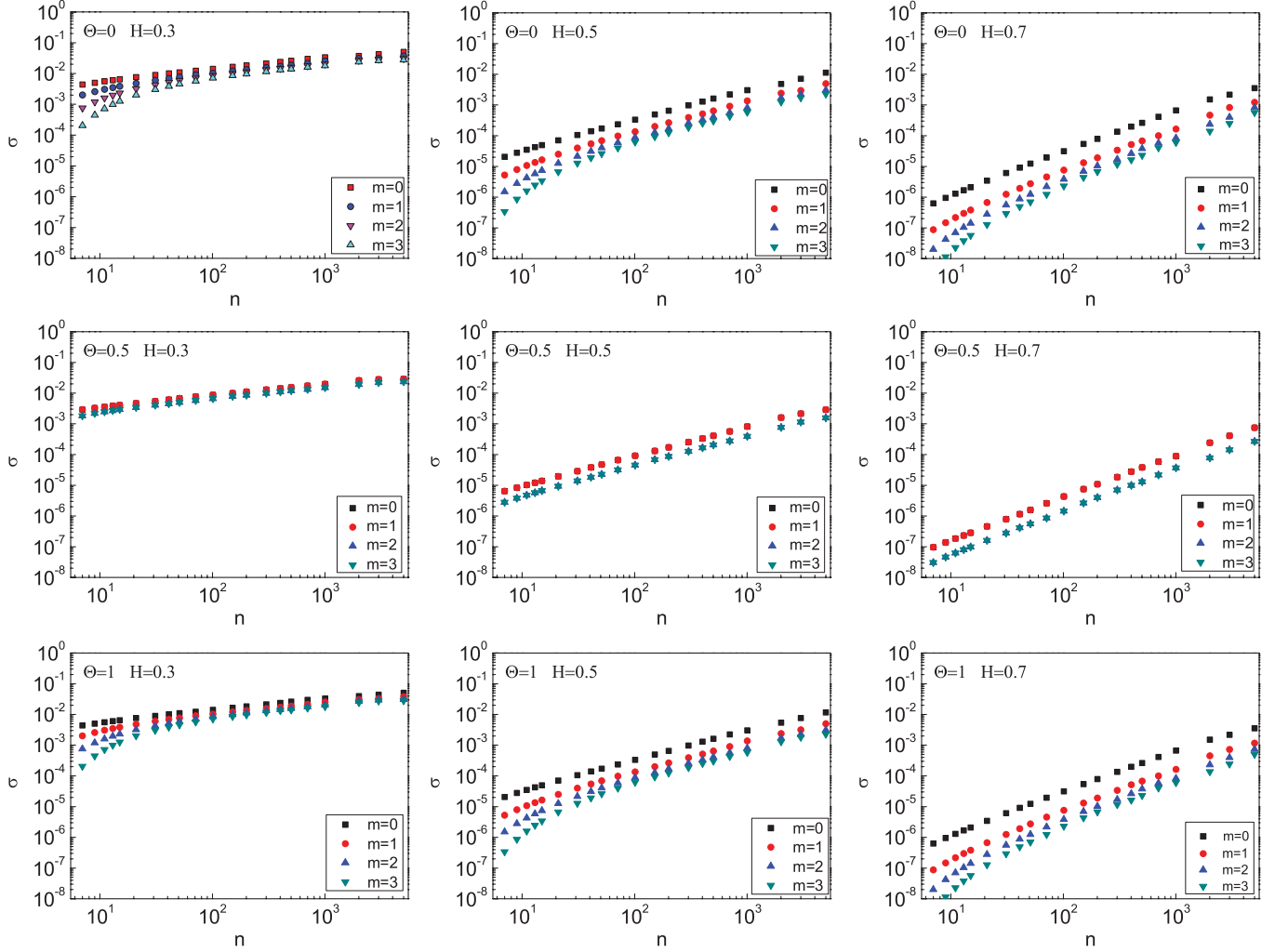


FIG. 2. (Color online) Log-log plots of σ_{DMA}^2 vs n for moving average polynomial degree $m = 0$, $m = 1$, $m = 2$, and $m = 3$, referred, respectively, to the endpoints ($\theta = 1$; $\theta = 0$) and to the midpoint ($\theta = 0.5$) of the window n . The series have been generated by the random midpoint displacement algorithm. The nominal Hurst exponent is $H = 0.3$, $H = 0.5$, and $H = 0.7$. The values of H obtained on five samples of such series are shown in Table I.

values of the Hurst exponents estimated as the slopes of the curves plotted in Fig. 2 are summarized in Table I. The length of the series is $N = 2^{20}$. In order to check the self-similarity of the moving average polynomials for shorter series, samples with length equal to $N = 2^{16}$, $N = 2^{14}$, $N = 2^{12}$, $N = 2^{10}$ with $H = 0.5$ have been analyzed for $\theta = 0.5$ and

$m = 0$, $m = 1$, $m = 2$, and $m = 3$. The results are shown in Table II.

The Hurst exponent is estimated through a linear best fit of the numerical data (similarly to those plotted in Fig. 2). Such a linear dependence does not hold exactly for small n , particularly for $\theta = 0$ and $\theta = 1$. The deviations occurring at

TABLE I. Estimation of the Hurst exponent and relative error.

		$m = 0$	ΔH_0	$m = 1$	ΔH_1	$m = 2$	ΔH_2	$m = 3$	ΔH_3
$H = 0.3$	$\theta = 0$	0.32	0.07	0.35	0.17	0.40	0.33	0.39	0.30
	$\theta = 0.5$	0.31	0.03	0.31	0.03	0.31	0.03	0.31	0.03
	$\theta = 1$	0.32	0.07	0.35	0.17	0.40	0.33	0.40	0.33
$H = 0.5$	$\theta = 0$	0.51	0.02	0.54	0.08	0.58	0.16	0.56	0.12
	$\theta = 0.5$	0.50	0.00	0.50	0.00	0.50	0.00	0.50	0.00
	$\theta = 1$	0.51	0.02	0.54	0.08	0.58	0.16	0.57	0.14
$H = 0.7$	$\theta = 0$	0.72	0.03	0.74	0.06	0.78	0.11	0.74	0.06
	$\theta = 0.5$	0.69	-0.01	0.69	-0.01	0.69	-0.01	0.69	-0.01
	$\theta = 1$	0.72	0.03	0.74	0.06	0.78	0.11	0.75	0.07

TABLE II. Estimation of the Hurst exponent for series with different length N with $H = 0.5$. The reference for the moving window is $\theta = 0.5$.

	$N = 2^{16}$	$N = 2^{14}$	$N = 2^{12}$	$N = 2^{10}$
$m = 0$	0.48	0.48	0.43	0.35
$m = 1$	0.48	0.48	0.43	0.35
$m = 2$	0.50	0.49	0.45	0.38
$m = 3$	0.50	0.49	0.45	0.38

short scales are quite generally reported for the zeroth order polynomials (see [40] and references therein). It is plausible that higher-order polynomials are more strongly affected by the nonlinearities, which may explain why the discrepancies

TABLE III. Asymptotic values of the DMA variances with $\tilde{y}_n(i)$ of order zero and one. The reference point is in the first point of the window ($\theta = 1$), in the midpoint ($\theta = 0.5$), and in the endpoint ($\theta = 0$). The factor n^{2H} has been omitted everywhere.

	σ_{DMA_0}	σ_{DMA_1}
$\theta = 0$	$\frac{1}{2(H+1)}$	$\frac{1-H}{(H+1)(H+2)}$
$\theta = 0.5$	$\frac{2^{1-2H}(H+1)-1}{2(H+1)(2H+1)}$	$\frac{2^{1-2H}(H+1)-1}{2(H+1)(2H+1)}$
$\theta = 1$	$\frac{1}{2(H+1)}$	$\frac{1-H}{(H+1)(H+2)}$

in the estimations of H increase with m . For $\theta = 0.5$, the data for $m = 0$ and $m = 1$ practically overlap, as well as those

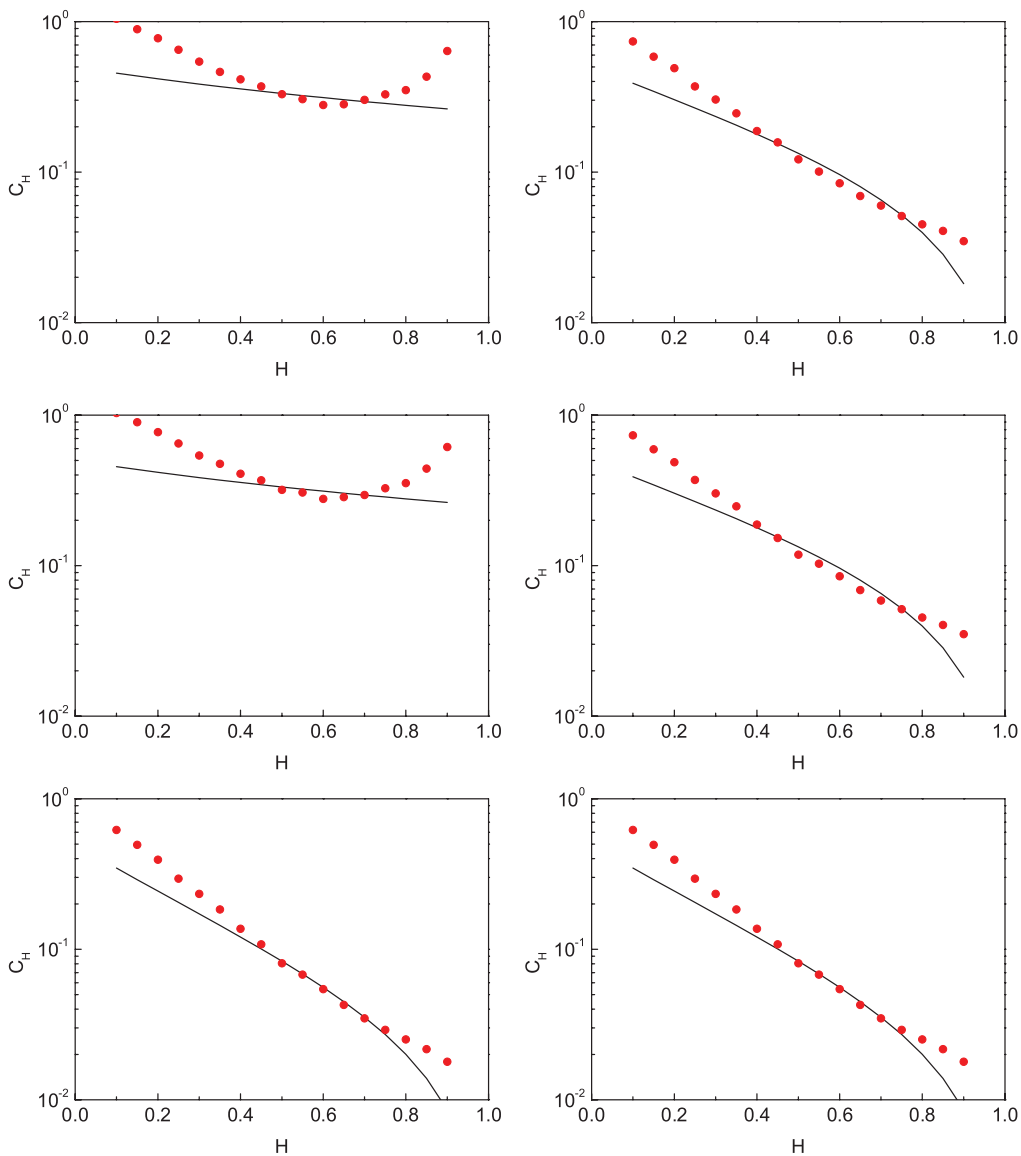


FIG. 3. (Color online) Prefactor C_H of the scaling laws (8) for $m = 0$ (left column) and $m = 1$ (right column), respectively, with $\theta = 1$, $\theta = 0.5$, and $\theta = 0$. Circles are numerical estimations obtained by using self-similar series generated by the random midpoint displacement algorithm. Continuous lines are analytical values obtained by using the C_H expressions given respectively by Eqs. (9a) and (9b). The different values of C_H at the extremes of the curves are due to the H overestimation in the linear fits of the curves plotted in Fig. 2. The errors can be estimated by the data of Table I where nominal and experimental values of H are reported.

for $m = 2$ and $m = 3$. This can be understood on the basis of the following reasoning. The moving average acts as a discrete integral over the series; since for $\theta = 0.5$ the reference point is in the center of the moving window, all the sums are performed over a symmetric interval. In this condition, the odd terms of the polynomials do not contribute to the sums, as can be inferred by thinking of the integral of odd functions over symmetric intervals. This cancellation mechanism may also explain the fact that low scale nonlinearities are smoothed out for $\theta = 0.5$, as shown in Fig. 2.

III. ASYMPTOTIC BEHAVIOR

In this section the asymptotic behavior of the generalized variance defined by Eq. (7) is investigated with $\tilde{y}_n(i)$ defined by Eq. (5) for $m = 1$. The asymptotic behavior of Eq. (7) yields a closed-form approximation of the scaling law of the form

$$\sigma_{\text{DMA}}^2 = C_H n^{2H} \quad (8)$$

at large n . The whole process is technically easy but quite cumbersome, thus more details are provided in the Appendix. The motivation for working out expression (8) is to prove that the self-similarity index of the time series is kept unchanged after implementing each step of the algorithm. This kind of investigation has been performed for the DFA in [44,45], for the DMA in [46], and for the R/S in [47]. We report three cases of particular interest extracted from Eq. (A16) of the Appendix:

$$\theta = 0; \theta = 1 \quad C_H = \frac{1-H}{(H+1)(H+2)}, \quad (9a)$$

$$\theta = 0.5 \quad C_H = \frac{1}{2(H+1)} - \frac{1-2^{-2H}}{2H+1}. \quad (9b)$$

In Table III the prefactors of the scaling laws (9a) and (9b) are summarized in the third column. In the second column those obtained for the zeroth order σ_{DMA}^2 are also reported [46].

As for the zeroth order σ_{DMA}^2 , the asymptotic values coincide at the endpoints of the moving window (i.e., with $\theta = 0$ and $\theta = 1$). For moving average polynomial referred to the middle of the window ($\theta = 0.5$), the zeroth and first order exhibit the same value of the variance. For $\theta = 0$ and $\theta = 1$, and in general $\forall \theta \neq 0.5$, the fit of order one is more accurate than that of order zero (the variance is smaller). Finally, we

compare the analytical results reported in the last column of Table III with those obtained by numerical estimation shown in Fig. 2. The behavior of the σ_{DMA}^2 expected from the asymptotic limit is in very good agreement with the numerical estimates. In Fig. 3 the theoretical values of C_H , calculated by using Eqs. (9a) and (9b), are compared with those obtained by the intercepts of the curves plotted in Fig. 2 for $\theta = 0$, $\theta = 0.5$, and $\theta = 1$. Since the fractional Brownian motions have been generated by the RMD algorithm, in the calculation of C_H it must be kept in mind that $\sigma^2 = (1 - 2^{2H-2})/2^{2H\nu} \sigma_{\text{Gauss}}^2$, ν being the number of steps and σ_{Gauss}^2 the variance defined for the RMD algorithm.

IV. CONCLUSIONS

The relationship for the calculation of the standard moving average Eq. (1) has been generalized allowing the definition of higher-order moving average polynomials Eqs. (5) and (6). The scaling behavior of such polynomials has been characterized by means of the detrending moving average algorithm. The proof of self-similarity rules out the existence of characteristic times and cut-off frequencies in the trend estimation. Furthermore, the asymptotic behavior of the exponents H of the moving average polynomials and of their detrending moving average variance agree, meaning that DMA algorithm does not change the value of H . The asymptotic values are compared with the results obtained by the simulations. The higher-order polynomials provide to trend estimates at smaller and smaller time scales. As the degree m of the polynomial increases, the low-frequency components are filtered out accordingly. Remarkably, polynomials with different degrees are obtained with constant moving average window n , thus trends at different time spans can be calculated over data set having the same size. These polynomials could improve the accuracy of trend estimates over different space or time horizons as needed for example in financial markets and image texture analysis.

APPENDIX: ASYMPTOTIC BEHAVIOR: DERIVATION OF THE EQUATIONS

We consider the coefficients $a_0(i)$ and $a_1(i)$ in their general form where the sum extremes contains the term θn , with θ a parameter ranging from 0 to 1,

$$\tilde{a}_1(i) = \frac{\sum_{k=-\theta n}^{n-1-\theta n} y(i-k)(i-k) - \frac{1}{n} \sum_{k=-\theta n}^{n-1-\theta n} y(i-k) \sum_{h=-\theta n}^{n-1-\theta n} (i-h)}{\sum_{k=-\theta n}^{n-1-\theta n} (i-k)^2 - \frac{1}{n} \left[\sum_{k=-\theta n}^{n-1-\theta n} (i-k) \right]^2}, \quad (A1a)$$

$$\tilde{a}_0(i) = \frac{1}{n} \sum_{k=-\theta n}^{n-1-\theta n} y(i-k) - \frac{1}{n} \tilde{a}_1(i) \sum_{k=-\theta n}^{n-1-\theta n} (i-k). \quad (A1b)$$

The coefficients $a_0(i)$ and $a_1(i)$ can be simplified and rewritten as

$$\tilde{a}_1(i) = \frac{12}{n^3} \left[\sum_{k=0}^{n-1} y(i-k)(i-k) + \left(\frac{n}{2} - i \right) \sum_{k=0}^{n-1} y(i-k) \right], \quad (A2a)$$

$$\tilde{a}_0(i) = \frac{1}{n} \sum_{k=0}^{n-1} y(i-k) + \frac{n}{2} \tilde{a}_1(i) - i \tilde{a}_1(i), \quad (A2b)$$

where the change of variables $k \rightarrow k + \theta n$ and $i \rightarrow i - \theta n$ has also been implemented. With these notations Eq. (7) becomes

$$\sigma_{\text{DMA}}^2 = \frac{1}{N-n} \sum_{i=n}^N [y(i-\theta n) - \tilde{a}_0(i) - (i-\theta n)\tilde{a}_1(i)]^2. \quad (\text{A3})$$

The procedure is now to substitute Eqs. (A2a) and (A2b) into (A3) and to compute all the summations in the large n limit, which formally amounts to replace summations with integrals.

$$\begin{aligned} (N-n)\sigma_{\text{DMA}}^2 &= \sum_{i=n}^N [y(i-\theta n) - a_0(i) - (i-\theta n)a_1(i)]^2 \\ &= \sum_{i=n}^N [y^2(i-\theta n) + a_0^2(i) + i^2 a_1^2(i) - 2a_0(i)y(i-\theta n) - 2ia_1(i)y(i-\theta n) + 2ia_0(i)a_1(i)] \\ &\quad + \sum_{i=n}^N [\theta^2 a_1^2(i) - 2\theta i a_1^2(i) + 2\theta a_1(i)y(i-\theta n) - 2\theta a_0(i)a_1(i)] \\ &= \sum_{i=n}^N y^2(i-\theta n) + \frac{16}{n^2} \sum_{i=n}^N \left[\sum_{k=0}^n y(i-k) \right]^2 + \frac{36}{n^4} \sum_{i=n}^N \left[\sum_{k=0}^n y(i-k)(i-k) \right]^2 \\ &\quad + \frac{36}{n^4} \sum_{i=n}^N i^2 \left[\sum_{k=0}^n y(i-k) \right]^2 - \frac{48}{n^3} \sum_{i=n}^N i \left[\sum_{k=0}^n y(i-k) \right]^2 \\ &\quad + \frac{48}{n^3} \sum_{i=n}^N \sum_{k=0}^n y(i-k)(i-k) \sum_{h=0}^n y(i-h) - \frac{72}{n^4} \sum_{i=n}^N i \sum_{k=0}^n y(i-k)(i-k) \sum_{h=0}^n y(i-h) \\ &\quad - \frac{8}{n} \sum_{i=n}^N y(i-\theta n) \sum_{k=0}^n y(i-k) - \frac{12}{n^2} \sum_{i=n}^N y(i-\theta n) \sum_{k=0}^n y(i-k)(i-k) \\ &\quad + \frac{12}{n^2} \sum_{i=n}^N i y(i-\theta n) \sum_{k=0}^n y(i-k) + \frac{144}{n^6} (\theta^2 n^2 - \theta n^2) \sum_{i=n}^N \left\{ \left[\sum_{k=0}^n y(i-k)(i-k) \right]^2 \right. \\ &\quad \left. + \left(\frac{n}{2} - i \right)^2 \left[\sum_{k=0}^n y(i-k) \right]^2 + 2 \left(\frac{n}{2} - i \right) \sum_{k=0}^n y(i-k)(i-k) \sum_{h=0}^n y(i-h) \right\} \\ &\quad + \frac{24}{n^2} \theta \sum_{i=n}^N \left\{ y(i-\theta n) \sum_{k=0}^n y(i-k)(i-k) + \left(\frac{n}{2} - i \right) y(i-\theta n) \sum_{k=0}^n y(i-k) \right. \\ &\quad \left. - \frac{1}{n} \sum_{k=0}^n y(i-k)(i-k) \sum_{h=0}^n y(i-h) - \frac{1}{n} \left(\frac{n}{2} - i \right) \left[\sum_{k=0}^n y(i-k) \right]^2 \right\}. \end{aligned} \quad (\text{A4})$$

Taking the large n limit ($n \rightarrow \infty$), while keeping $n \ll N$, of Eq. (A4) implies that we can approximate summations with integrals:

$$\begin{aligned} \sum_{i=n}^N &\simeq n \int_1^{\frac{N}{n}} dx, \quad \text{with } i = nx, \\ \sum_{k=0}^n &\simeq n \int_0^1 dx, \quad \text{with } k = nx. \end{aligned} \quad (\text{A5})$$

It is convenient to compute each sum separately, and then substitute the results into (A4). For the sake of clarity, let us stress that in the following equations the equality signs are intended up to higher-order corrections in the large n expansion:

$$\sum_{i=n}^N y^2(i-\theta n) = \frac{n^{2H+1}}{2H+1} \left[\left(\frac{N}{n} - \theta \right)^{2H+1} - (1-\theta)^{2H+1} \right], \quad (\text{A6})$$

$$\sum_{i=n}^N \left[\sum_{k=0}^n y(i-k) \right]^2 = \frac{n}{2(H+1)(2H+1)} [N^{2H+2} - n^{2H+2} - (N-n)^{2H+2}] - \frac{n^{2H+2}}{2(H+1)(2H+1)} (N-n), \quad (\text{A7})$$

$$\begin{aligned} \sum_{i=n}^N i \left[\sum_{k=0}^n y(i-k) \right]^2 &= \frac{n}{(2H+1)(2H+3)} [N^{2H+3} - n^{2H+3} - (N-n)^{2H+3}] \\ &\quad - \frac{n^2}{2(H+1)(2H+1)} (N-n)^{2H+2} - \frac{n^{2H+2}}{4(H+1)(2H+1)} (N^2 - n^2), \end{aligned} \quad (\text{A8})$$

$$\begin{aligned} \sum_{i=n}^N i^2 \left[\sum_{k=0}^n y(i-k) \right]^2 &= \frac{n}{2(2H+1)(H+2)} [N^{2H+4} - n^{2H+4} - (N-n)^{2H+4}] - \frac{2n^2}{(2H+1)(2H+3)} (N-n)^{2H+3} \\ &\quad - \frac{n^3}{2(H+1)(2H+1)} (N-n)^{2H+2} - \frac{n^{2H+2}}{6(H+1)(2H+1)} (N^3 - n^3), \end{aligned} \quad (\text{A9})$$

$$\begin{aligned} \sum_{i=n}^N \left[\sum_{k=0}^n y(i-k)(i-k) \right]^2 &= \frac{n}{4(H+1)(H+2)} [N^{2H+4} - n^{2H+4} - (N-n)^{2H+4}] - \frac{n^2}{2(H+1)(2H+3)} (N-n)^{2H+3} \\ &\quad - \frac{n^{2H+2}}{6(H+1)(2H+1)} (N^3 - n^3) - \frac{n^2}{4(H+1)(2H+3)} [N^{2H+3} - n^{2H+3} - (N-n)^{2H+3}] \\ &\quad + \frac{n^{2H+3}}{4(H+1)(2H+1)} (N^2 - n^2) - \frac{n^{2H+4}}{4(H+1)(2H+1)(H+2)} (N-n), \end{aligned} \quad (\text{A10})$$

$$\begin{aligned} \sum_{i=n}^N \left[\sum_{k=0}^n \sum_{h=0}^n y(i-k)(i-k)y(i-h) \right] &= \frac{n}{4(H+1)(2H+3)} [N^{2H+3} - n^{2H+3} - (N-n)^{2H+3}] + \frac{n}{2(2H+1)(2H+3)} \\ &\quad \times [N^{2H+3} - n^{2H+3} - (N-n)^{2H+3}] - \frac{n^2}{4(H+1)(2H+1)} (N-n)^{2H+2} \\ &\quad - \frac{n^2}{8(H+1)(2H+1)} [N^{2H+2} - n^{2H+2} - (N-n)^{2H+2}] - \frac{n^{2H+2}}{4(H+1)(2H+1)} \\ &\quad \times (N^2 - n^2) + \frac{n^{2H+3}}{4(H+1)(2H+1)} (N-n), \end{aligned} \quad (\text{A11})$$

$$\begin{aligned} \sum_{i=n}^N \left[\sum_{k=0}^n \sum_{h=0}^n iy(i-k)(i-k)y(i-h) \right] &= \frac{n}{8(H+1)(H+2)} [N^{2H+4} - n^{2H+4} - (N-n)^{2H+4}] - \frac{n^2}{4(H+1)(2H+3)} \\ &\quad \times (N-n)^{2H+3} + \frac{n}{4(2H+1)(H+2)} [N^{2H+4} - n^{2H+4} - (N-n)^{2H+4}] \\ &\quad - \frac{n^2}{(2H+1)(2H+3)} (N-n)^{2H+3} - \frac{n^3}{8(H+1)(2H+1)} (N-n)^{2H+2} \\ &\quad - \frac{n^2}{4(2H+1)(2H+3)} [N^{2H+3} - n^{2H+3} - (N-n)^{2H+3}] \\ &\quad - \frac{n^{2H+2}}{6(H+1)(2H+1)} (N^3 - n^3) + \frac{n^{2H+3}}{8(H+1)(2H+1)} (N^2 - n^2), \end{aligned} \quad (\text{A12})$$

$$\begin{aligned} \sum_{i=n}^N \left[\sum_{k=0}^n y(i-\theta)y(i-k) \right] &= \frac{n}{2(2H+1)} [(N-\theta)^{2H+1} - (n-\theta)^{2H+1}] + \frac{n}{4(H+1)(2H+1)} \\ &\quad \times [N^{2H+2} - n^{2H+2} - (N-n)^{2H+2}] - \frac{1}{2(2H+1)} [(n-\theta)^{2H+1} + \theta^{2H+1}] (N-n), \end{aligned} \quad (\text{A13})$$

$$\begin{aligned}
 & \sum_{i=n}^N \left[\sum_{k=0}^n y(i-\theta)y(i-k)(i-k) \right] \\
 &= \frac{1}{4(H+1)(2H+3)} [N^{2H+3} - n^{2H+3} - (N-n)^{2H+3}] - \frac{N^2}{4(2H+1)} [(N-\theta)^{2H+1} - (n-\theta)^{2H+1}] \\
 &+ \frac{n}{4(H+1)} [(N-\theta)^{2H+2} - (n-\theta)^{2H+2}] + \frac{n\theta}{2(2H+1)} [(N-\theta)^{2H+1} - (n-\theta)^{2H+1}] - \frac{(n-\theta)^{2H+1}}{4(2H+1)} (N^2 - n^2) \\
 &+ \frac{\theta(n-\theta)^{2H+1}}{2(2H+1)} (N-n) + \frac{(n-\theta)^{2H+2}}{4(H+1)} (N-n) - \frac{\theta^{2H+1}}{4(2H+1)} (N^2 - n^2) + \frac{\theta^{2H+2}}{2(2H+1)} (N-n) - \frac{\theta^{2H+2}}{4(H+1)} (N-n),
 \end{aligned} \tag{A14}$$

$$\begin{aligned}
 & \sum_{i=n}^N \left[\sum_{k=0}^n y(i-\theta)(i-\theta)y(i-k) \right] \\
 &= \frac{n}{4(H+1)} [(N-\theta)^{2H+2} - (n-\theta)^{2H+2}] + \frac{1}{2(2H+1)(2H+3)} [N^{2H+3} - n^{2H+3} - (N-n)^{2H+3}] \\
 &- \frac{\theta}{4(H+1)(2H+1)} [N^{2H+2} - n^{2H+2} - (N-n)^{2H+2}] - \frac{n}{4(H+1)(2H+1)} (N-n)^{2H+2} - \frac{(n-\theta)^{2H+1}}{4(2H+1)} (N^2 - n^2) \\
 &+ \frac{\theta(n-\theta)^{2H+1}}{2(2H+1)} (N-n) - \frac{\theta^{2H+1}}{4(2H+1)} (N^2 - n^2) + \frac{\theta^{2H+2}}{2(2H+1)} (N-n) + \frac{n\theta}{2(2H+1)} [(N-\theta)^{2H+1} - (n-\theta)^{2H+1}] \\
 &- \frac{\theta}{2(2H+1)} [(N-\theta)^{2H+1} - (n-\theta)^{2H+1}] (N-n) + \frac{\theta}{4(H+1)(2H+1)} [N^{2H+2} - n^{2H+2} - (N-n)^{2H+2}].
 \end{aligned} \tag{A15}$$

Plugging all these partial results into Eq. (A4), after some algebra one obtains

$$\begin{aligned}
 & n^{-2H} \sigma_{\text{DMA}}^2 \\
 &= \frac{4}{(H+1)(H+2)} - \frac{9}{(H+1)(H+2)(2H+1)} + \frac{4}{2H+1} [\theta^{2H+1} + (1-\theta)^{2H+1}] + \frac{3}{H+1} [\theta^{2H+2} - (1-\theta)^{2H+2}] \\
 &- \frac{6}{2H+1} \theta(1-\theta)^{2H+1} - \frac{6}{2H+1} \alpha^{2H+2} + \frac{18H}{(H+1)(H+2)(2H+1)} \theta(\theta-1) + \frac{6}{H+1} \theta(1-\theta)^{2H+2} \\
 &+ \frac{6}{(H+1)(2H+1)} \theta^{2H+3} - \frac{6}{2H+1} \theta^{2H+2} - \frac{6}{2H+1} \theta(1-\theta)^{2H+1} + \frac{12}{2H+1} \theta^2(1-\theta)^{2H+1}.
 \end{aligned} \tag{A16}$$

[1] H. Erzgraber *et al.*, *Physica A* **387**, 6567 (2008).
 [2] T. DiMatteo, *Quant. Finan.* **7**, 21 (2007).
 [3] A. Carbone, G. Castelli, and H. E. Stanley, *Physica A* **344**, 267 (2004).
 [4] A. W. Lo, H. Mamaysky, and J. Wang, *J. Finan.* **55**, 1705 (2000).
 [5] L. Menkhoff, *J. Bank. Finan.* **34**, 2573 (2010).
 [6] F. A. Longstaff and E. S. Schwartz, *Rev. Finan. Stud.* **14**, 113 (2001).
 [7] M. Dai, P. Li, and J. E. Zhang, *J. Econ. Dyn. Control* **34**, 542 (2010).
 [8] E. Bullmore *et al.*, *Human Brain Mapping* **12**, 61 (2001).
 [9] F. Crevecoeur, B. Bollens, C. Detrembleur, and T. M. Lejeune, *J. Neurosci. Meth.* **192**, 163 (2010).
 [10] A. M. Wink *et al.*, *Human Brain Mapping* **29**, 791 (2008).
 [11] V. Maxim *et al.*, *Neuroimage* **25**, 141 (2005).
 [12] A. Kilcik *et al.*, *Astrophys. J.* **693**, 1173 (2009).
 [13] M. S. Movahed *et al.*, *J. Stat. Mech. Theo. Exp.* (2006) P02003.
 [14] E. Koscielny-Bunde *et al.*, *J. Hydrol.* **322**, 120 (2006).
 [15] A. Carbone, B. M. Chiaia, B. Frigo, and C. Türk, *Phys. Rev. E* **82**, 036103 (2010).
 [16] W. S. Lam, W. Ray, P. N. Guzdar, and R. Roy, *Phys. Rev. Lett.* **94**, 010602 (2005).
 [17] L. Lacasa *et al.*, *Europhys. Lett.* **86**, 30001 (2009).
 [18] J. Mielniczuk and P. Wojdylo, *Comp. Stat. Data Anal.* **51**, 4510 (2007).
 [19] D. Delignieres *et al.*, *J. Math. Psych.* **50**, 525 (2006).
 [20] P. Oswiecimka, J. Kwapien, and S. Drozd, *Phys. Rev. E* **74**, 016103 (2006).
 [21] C.-K. Peng, S. V. Buldyrev, S. Havlin, M. Simons, H. E. Stanley, and A. L. Goldberger, *Phys. Rev. E* **49**, 1685 (1994).
 [22] C. Heneghan and G. McDarby, *Phys. Rev. E* **62**, 6103 (2000).
 [23] K. Hu, P. C. Ivanov, Z. Chen, P. Carpena, and H. E. Stanley, *Phys. Rev. E* **64**, 011114 (2001).
 [24] Z. Chen, P. C. Ivanov, K. Hu, and H. E. Stanley, *Phys. Rev. E* **65**, 041107 (2002).
 [25] R. O. Weber and P. Talkner, *J. Geophys. Res.* **106**, 20131 (2001).
 [26] J. W. Kantelhardt *et al.*, *Physica A* **316**, 87 (2002).
 [27] A. Castro e Silva and J. G. Moreira, *Physica A* **235**, 327 (1997).
 [28] N. Vandewalle and M. Ausloos, *Phys. Rev. E* **58**, 6832 (1998).

- [29] E. Alessio, A. Carbone, G. Castelli, and V. Frappietro, *Eur. J. Phys. B* **27**, 197 (2002).
- [30] A. Carbone, G. Castelli, and H. E. Stanley, *Phys. Rev. E* **69**, 026105 (2004).
- [31] J. Alvarez-Ramirez, E. Rodriguez, and J. C. Echeverria, *Physica A* **354**, 199 (2005).
- [32] G. F. Gu and W. X. Zhou, *Phys. Rev. E* **82**, 011136 (2010).
- [33] D. Grech and Z. Mazur, *Acta Phys. Pol. B* **36**, 2403 (2005).
- [34] L. M. Xu, P. C. Ivanov, K. Hu, Z. Chen, A. Carbone, and H. E. Stanley, *Phys. Rev. E* **71**, 051101 (2005).
- [35] A. Bashan, R. Bartsch, J. W. Kantelhardt, and S. Havlin, *Physica A* **387**, 5080 (2008).
- [36] Q. D. Y Ma, R. P. Bartsch, P. Bernaola-Galvan, M. Yoneyama, and P. C. Ivanov, *Phys. Rev. E* **81**, 031101 (2010).
- [37] S. Drozd, J. Kwapien, P. Oswiecimka, and R. Rak, *Europhys. Lett.* **88**, 60003 (2009).
- [38] B. Podobnik and H. E. Stanley, *Phys. Rev. Lett.* **100**, 084102 (2008).
- [39] S. Arianos and A. Carbone, *J. Stat. Mech. Theo. Exp.* (2009) P03037.
- [40] A. Carbone, *Phys. Rev. E* **76**, 056703 (2007).
- [41] G. F. Gu and W. X. Zhou, *Phys. Rev. E* **74**, 061104 (2006).
- [42] C. Türk, A. Carbone, and B. M. Chiaia, *Phys. Rev. E* **81**, 026706 (2010).
- [43] W. X. Zhou and D. Sornette, *Int. J. Mod. Phys. C* **13**, 137 (2002).
- [44] M. S. Taqqu, V. Teverovsky, and W. Willinger, *Fractals* **3**, 785 (1995).
- [45] G. M. Raymond and J. B. Bassingthwaighte, *Physica A* **265**, 85 (1999).
- [46] S. Arianos and A. Carbone, *Physica A* **382**, 9 (2007).
- [47] W. Li, C. Yu, A. Carriquiry, and W. Kliemann, *Stat. Prob. Lett.* **81**, 83 (2011).